Superconducting Tunnel Junctions

Shantanu Jha and Chris West
(Dated: February 12$^{\text{th}}$, 2019)

When cooled to extreme temperatures, some metals exhibit superconducting behavior that change the available energy states of electrons. In practice, this means a finite voltage difference is required between two metals to observe a current flow. This superconducting gap in energy states is a characteristic property of a metal. Here, we measure the gap of lead and aluminum, finding values of (VALUE) and (VALUE), respectively. Compared to the accepted values of (VALUE) and (VALUE), we are impressed with our results. We also qualitatively explore the results predicted by Bardeen-Cooper-Schrieffer (BCS) theory, in which superconductivity causes a condensation of cooper pairs into a boson-like state - allowing these pairs of electrons to tunnel together, something that would be extremely unlikely if only considering regular quantum tunneling probability.

I. INTRODUCTION

In this experiment, we measure the superconducting gap of two metals, lead and aluminum. To this end, we collect three sets of data at different temperatures. A thorough χ^2 minimization process will compare our results to theory, and find the experimental values for the superconducting gaps, Δ_{Pb} and Δ_{Al}.

In order to isolate the effects of the superconducting gap of each metal, we aim to examine three junction regimes with respect to the state (normal / superconducting) of the two metals; normal - insulator - normal (NIN), superconducting - insulator - normal (SIN), and superconducting - insulator - superconducting (SIS).

A. NIN

When both metals are at room temperature (well above their critical temperatures), we have the NIN regime. Fig. I.1 (a) shows the possible energy states when zero voltage is applied. There is tunnelling occurring, but electrons tunneling from lead to aluminum cancel those tunneling from aluminum to lead, resulting in zero current. When a voltage is applied, the baseline voltage difference between the metals changes and results in, for example, electrons on the left being able to tunnel to the right with much higher probability than in the other direction - and thus, a current flow. For the NIN regime, the expected $I(V)$ equation is

$$I_{NIN} = \frac{V}{R_o} \qquad (\text{I.1})$$

where

$$R_o = \frac{1}{eA|\mathcal{T}|^2 N_{Ln}(0) N_{Rn}(0)} \ . \qquad (\text{I.2})$$

$|\mathcal{T}^2|$ is the tunneling probability and A is a proportionality constant related to the geometry of the junction. N_{Ln} and N_{Rn} are the density of states of the left (L) and right (R) metals at normal (n) (temperature-wise) conditions, and are evaluated here at energy $E = 0$. Since Eq. I.2 is a temperature-independent constant, Eq. I.1 is linear.
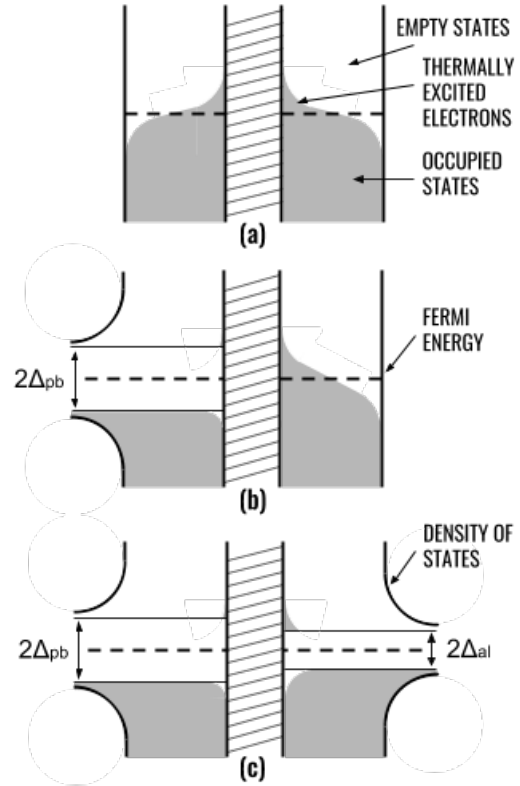

Figure I.1. Possible energy states at zero voltage for the (a) NIN, (b) SIN, and (c) SIS regimes. Lead is on the left and aluminum is on the right, separated by an insulating barrier. Adapted from [2].

B. SIN

When the temperature of the apparatus is cooled below $7.2K$ (the critical temperature of lead), we enter the SIN regime. Fig. I.1 (b) shows the possible energy states when zero voltage is applied. The superconducting gap creates a band of energy levels that no electrons may occupy. Thus, at zero voltage there is no tunneling occurring. After a small increase in voltage, the picture won't have changed much, and still no current will flow. Finally, after there is enough of a voltage difference for
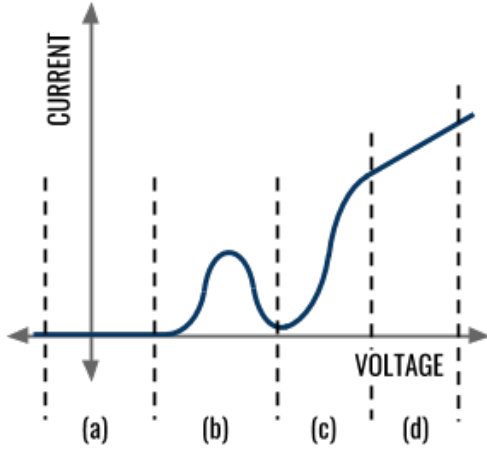
Figure I.2. A graph of the theory prediction for the $I(V)$ curve of the SIS regime at nonzero temperature.

the normal metal (aluminum, in this case) to have electrons at energy levels equal to the energy levels of the holes of lead tunneling will begin, and current will flow. Graphically, we expect a $I(V)$ curve to be constant at zero until $V = \Delta_{Pb}/e$, at which point the current will spike up to the underlying linear value, as shown in Fig. I.2 (c) and (d). The expected $I(V)$ equation is

$$I_{SIN} = \frac{1}{eR_o} \int_{-\infty}^{+\infty} \frac{N_{Ls}(E)}{N_{Ln}(0)} [f(E) - f(E+eV)]dE \ . \quad (I.3)$$

C. SIS

Finally, below $1.2\,\mathrm{K}$ (the critical temperature of aluminum[1]) is described by the SIS regime. Similar to the SIN regime, tunneling (and thus current) is prohibited from flowing at zero voltage due to the gaps in possible energy states for both metals (as shown in Fig. I.1 (c)). Theory predicts the $I(V)$ curve in Fig. I.2. Current does not start to flow until $V = (\Delta_{al} - \Delta_{pb})/e$ when electrons that have "smeared" above the gap of aluminum have available spots in lead that they can tunnel to. Further increase, though, causes a decrease in voltage, as any "smeared" aluminum electrons are now at higher any levels than the available states in lead. Finally, at $V = (\Delta_{Al} + \Delta_{Pb})/e$, the gaps of the two metals are no longer overlapping, and we see the same jump in voltage as in the SIN regime. The expected $I(V)$ equation is

$$I_{SIS} = \frac{1}{eR_o} \int_{-\infty}^{+\infty} \frac{N_{Ls}(E)}{N_{Ln}(0)} \frac{N_{Rs}(E+ev)}{N_{Rn}(0)}$$
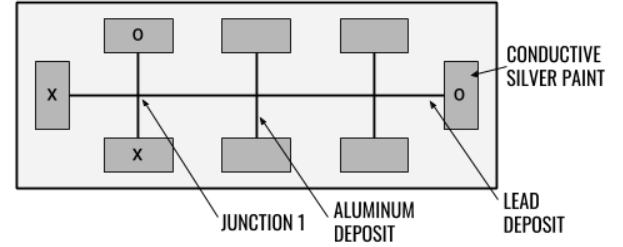$$[f(E) - f(E+eV)]dE \ . \quad (I.4)$$

Figure II.1. A diagram of a slide. The x's and o's indicate the four-point probe connections for Junction 1.

II. EXPERIMENTAL PROCEDURE

A. Preparation

In order to minimize contamination of the junctions, we prepared six slides - each with three junctions - using thermal evaporation. Fig. II.1 shows a diagram of a single slide. The lead layer was $4.08\,\mathrm{k\AA}$ thick and the aluminum layer was $1.06\,\mathrm{k\AA}$ thick. The slides were oxidized for approximately 6 minutes between deposition of the aluminum and the lead.

Of the six slides, a single one was chosen by roughly measuring the voltages between several contacts on each slide. We chose the slide that had the most consistent voltage differentials between symmetric contacts. The slide was tested again before data collection to ensure that the junctions had not degraded in the days between deposition and data collection.

B. Data Collection

Since the resistances of the junctions are all small, it is easier to vary current and measure voltage than vice versa. The computer will generate a voltage that will be converted to a predictable current at the large internal resistor R_v. Then the voltage across the junction is measured with a four-point probe to reduce voltage lost across the lead and aluminum wires. The upshot is that our data collection actually results in a $V(I)$ curve. Under normal conditions $I(V)$ is a bijective function, and thus can be inverted. However, for the SIS regime, we expect the behavior shown in Fig. I.2, which is notably not a function when the axis are flipped. This will give rise to hysteresis. Since we will be sweeping voltage in both the positive and negative directions, the domain of voltages that we aren't able to collect current data for will be minimal.

For the NIN regime, the chosen slide was loaded in the apparatus (depicted in Fig. II.2) and measurements of the three junctions were taken. For each junction voltage was varied from $-5\,\mathrm{V}$ to $5\,\mathrm{V}$ in a step size of $0.02\,\mathrm{V}$ in both the negative and positive directions. The sampling rate was $10,000$ samples/sec and we collected samples

for .01 seconds at each voltage. The frequency filter was set to 1000 Hz and the gain was set to 100. The internal resistor was set to $R_v = 10\,000\,\Omega$. These settings were not changed for the other regimes unless noted. All three junctions resulted in a linear set of data, with junction 1 being best fit by a line of slope (J1 SLOPE) (corresponding to R_o in Eq. I.1), junction 2 by a line of slope (J2 SLOPE), and J3 by a line of slope (J3 SLOPE). Given the consistency of these three values and their magnitude on the order of $10^1\Omega$, we felt comfortable continuing to the next regimes with this slide.

To get to the SIN regime, the liquid nitrogen and liquid helium were poured into the apparatus. The first junction was destroyed during the temperature change, but the second and third remained functioning well. The gain was increased to 500 and the internal resistor was switched to $100\,000\,\Omega$. For each junction, the voltage was varied from $-5\,V$ to $5\,V$ in a step size of $0.02\,V$ in both the negative and positive directions. The expected zero current behavior was observed for small voltages. The data from both the positive and negative sweeps of junction 2 are plotted together in Fig. (REFERENCE).

Finally, to get to the SIS regime, the pressure in the apparatus was decreased with a roughing pump. The pressure in the innermost chamber was monitored, and we began collecting data at 1.684 Torr. The second and third junctions functioned well after the temperature change was complete. The gain stayed at 500 and the internal resistor at $100\,000\,\Omega$. For each junction voltage was varied from $-1\,V$ to $1\,V$ in a step size of $0.004\,V$ in both the negative and positive directions. The smaller step size was selected in order to get greater clarity of the hysteresis effect. The smaller voltage range was selected to minimize the run time of the collection. The expected hysteresis effect was observed in both cases. The data from both the positive and negative sweeps of junction 2 are plotted together in Fig. (REFERENCE).

~~COMMENT ON BCS??~~

~~plot data?? (for any of these (NIN, SIN, SIS) or all)~~

III.   DATA ANALYSIS

A.   Error Analysis

1.   Sources of Error

Before we display our results, we will explain the meticulous error analysis this data has undergone.

As mentioned, our independent variable in this experiment was the current we send through our junction. This resulted in a $V(I)$ curve where the voltage across our junction V_j was measured as a function of the current across our junction I_j. In practice, it is important to note that we were able to construct a current across our junction I_j with our internal resistor R_v. Namely, we divided our circuit driving voltage V_{tot} by our very large internal resistance $R_v \approx R_{tot}$, which was approximately
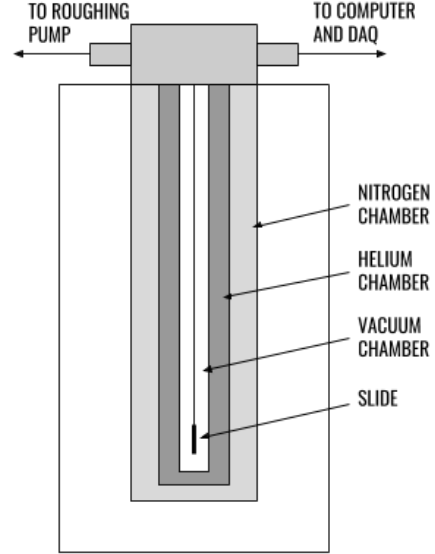

Figure II.2. A diagram of the cryostat.

our circuits total resistance, to find the total current going through our circuit $I_{tot} = I_j$, which was equal to the current going through our junction. Thus, by the error propagation formula, we have the relation:

$$I_j = \frac{V_{tot}}{R_v}, \ \delta I_j = \sqrt{\left(\frac{1}{R_v}\delta V_{tot}\right)^2 + \left(\frac{V_{tot}}{R_v^2}\delta R_v\right)^2} \ \text{(III.1)}$$

We estimated our $\delta R_v = .02R_v$ for a lack of a more precise measure of this internal resistor resistance. Our process to find δV_{tot}, the finite precision uncertainty of the voltages provided by our data acquisition system, is elaborated upon in section V A. After this process, we calculated a $\delta V_{tot} = .005V$, which we then used to find δI_j.

The calculations for the error bars of our measured junction voltages at a range of currents across our junction is similar to that of our horizontal error bars around our $V(I)$ curve. Since we collected a large amount of samples at every time step, at every driving current I_j, we were able to calculate δV_j from the standard deviation of our distribution of samples at every time step. We believe that this standard deviation of our samples at each time step included the effects of the finite resolution of each measurement, one that we also measured to be .005V. For this reason, we did not feel the need to separately include the finite resolution of each sample measurement in a calculation of the error bars of V_j.

Finally, we found a constant V_j offset in our data that we felt compelled to correct. The trials that we ran to determine the dependence, or lack thereof, of this offset on parameters such as gain, frequency filter settings, R_v

setting, and more helped us decide how to address this systematic offset. After much testing, we found that this offset occurred in a portion of our circuit inaccessible to us and before our amplification of the V_j signal. The trials through we confirmed the constant nature of this offset are stated in V A.

In this way, we were able to calculate the horizontal (δI_j) and vertical (δV_j) error bars of our $V(I)$ curve.

2. Error Propagation

The next step in our analysis involved taking our $V(I)$ curve and flipping both its points and the associated error bars to obtain a $I(V)$ curve.

We then aimed to include both the horizontal and vertical error bars in our error analysis calculations. We did this by first propagated our horizontal error bar (δV_j) in our $I(V)$ curve into associated vertical (δV_j) error bars. Then we added in quadrature our original vertical error bars (δV_j) and the error bars we had calculated by propagating our horizontal error bars (δI_j).

It is generally true that $\delta f(x) = \frac{\partial f(x)}{\partial x} \delta x$. We used this relation and the *approximately* linear resistor nature of our junctions in every regime (NIN, SIN, SIS) at large voltage ranges to simplify the $f(x)$ describing our $I(V)$ curve. This was a necessary step in propagating our horizontal error bars into something that could contribute towards our vertical error bars. Specifically, we assumed that:

$$I_j = \underbrace{\frac{1}{R_j}}_{m=\text{ slope}} V_j \qquad \text{(III.2)}$$

This relation allowed us to find the effective junction resistance of our junctions by linearly fitting the data we collected. By calculating the line of best fit for our $I(V)$ curves we were able to find $R_j = \frac{1}{m}$. This calculation of $R_j \pm \delta R_j$ then gave us an approximation for our $I(V)$ curve in any regime. We then used this approximation to calculate the propagation of our horizontal error bars to vertical error bars, in the following way:

$$\delta I(V)_{\text{horizontal}} = \sqrt{\left(\frac{V_j}{R_j^2}\delta R_j\right)^2 + \left(\frac{1}{R_j}\delta V_j\right)^2} \quad \text{(III.3)}$$

Lastly, we added these two vertical error bar contributions in quadrature.

$$\delta I(V)_{\text{tot}} = \sqrt{(\delta I_{\text{horizontal}})^2 + (\delta I_{\text{vertical}})^2} \qquad \text{(III.4)}$$

B. Reduced χ^2

While we were able to account for statistical errors at each point of our measurement record by using vertical error bars (δI_j), there are systematic errors and fit parameters in our theory that we must optimize and account for to get the best possible theoretical fit curve to compare to our data. These fit parameters also contain useful information about the nature of the materials used in our experiment, as we will soon see.

1. Free Fit Parameters

Namely, these free fit parameters include $R_\parallel$, $\delta_{\text{Pb}}, \delta_{\text{Al}}$, T, and R_0. $R_\parallel$ is a parameter that arise from the presence of a large but finite resistance in parallel with our junction or a small by nonzero resistance in series with our junction, both of which can smear out our $I(V)$.

δ_{Pb} and δ_{Al} represent the superconducting energy band levels that open up between allowed electron states when Pb and Al become superconducting respectively.

T is the temperature of our junction and R_0 is a temperature independent constant roughly related to the approximate linear resistance of our junction at any regime. In the NIN regime, R_0 is exactly equal to R_j, which is the slope of the NIN $I(V)$ curve.

While we can calculate R_0 for each junction through our experiments in the NIN regime, we must try to fit R, δ_{Pb}, δ_{Al}, and T to find the theoretical curves $I(V)$ closest to our experimental $I(V)$ curves in the SIN and SIS regimes respectively.

2. Reduced χ^2 Minimization

A common measured used to find fit parameters that minimize the deviation of experimental values from theoretical predictions is the reduced χ^2 metric. This metric can be roughly thought of as the distance between the experimental curve and the theoretical curve. Clearly, as we adjust the fit parameters that determine this theoretical curve, our reduced χ^2 measure will change to reflect the closeness or distance between the changing theoretical curve and static experimental curve. Thus, if we traverse a relevant parameter space and calculate this reduced χ^2 value for enough points on this space, we will be able to find the point in our parameter space that minimizes our reduced χ^2 and gets our theoretical curve as close as possible to our experimental curve. Formally, our reduced χ^2 can be written as χ^2_ν and calculated as follows:

$$\chi^2_\nu = \frac{1}{\nu} \underbrace{\sum_{i=1}^{N} \frac{(y_i - f(x_i, \alpha))^2}{\sigma_i}}_{\chi^2} \qquad \text{(III.5)}$$

where y_i are the N experimental data points, $f(x_i, \alpha)$ are the y values of our theoretical curve given parameters α, and σ_i is the uncertainty in y_i. In addition, $\nu = N - p$ is the number of data points N minus number of parameters p we are free to change. This ν reflects

the true degrees of freedom our experimental graph may have. The greater the degrees of freedom, the larger the ν we have to divide our χ^2 by to get a true measure of how close our experimental curve is to our theoretical curve given some parameters α. In other words, we are more forgiving of larger χ^2 values if there are more degrees of freedom ν for our experimental curve to differ from our theoretical curve on.

In summary, we will explore a grid of parameter choices and choose the one that minimizes our χ^2_ν measure. This will leave us with the theoretical $I(V)$ curve closest to our experimental data; in turn, we will be able to find the best estimates of our fit parameters. The closer our χ^2_ν is to 1 the better. $\chi^2_\nu < 1$ implies over-fitting, and $\chi^2_\nu >> 1$ implies the inaccuracy of our model.

3. Initial Parameter Estimation

4. Optimal Parameters with Uncertainty

5. Residuals

6. Frequency Filter: Further Reducing χ^2

C. Results

Important plots:
NIN data with L.O.B.F.
SIN data with BF curve
SIS data with BF curve
plot of residuals for one of these?

[We are currently working through what we believe to be a unit error in our χ^2_ν minimization. This is why we have not yet included our theoretical fit curves and adjoining fit parameter values in this draft.]
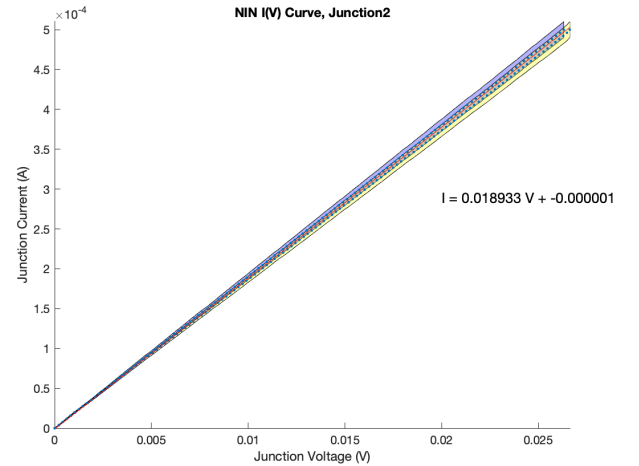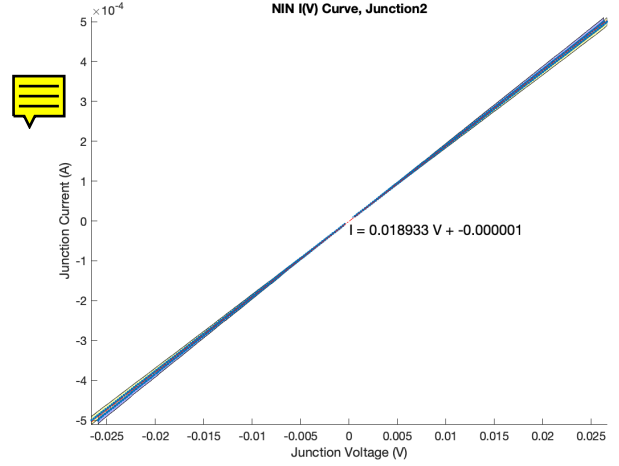
1. sec:3.3.1 NIN

2. sec:3.3.2 SIN

3. sec:3.3.3 SIS

IV. CONCLUSION

Having reduced our χ^2 to (CHI-SQUARE) for the SIN regime and to (CHI-SQUARE) for the SIS regime, we feel (confidence interval?) confident in our results. As such, we predict the superconducting gap of lead to be (LEAD GAP) and the superconducting gap of aluminum to be (AL GAP). These results are, respectively, (PERCENT ERROR) and (PERCENT ERROR) off from what theory predicts.

Given the largely pedagogical motivation for this experiment, there are many instances where more care

NIN I(V) Curve, Junction2

I = 0.018933 V + -0.000001

NIN I(V) Curve, Junction2

I = 0.018933 V + -0.000001

could have been taken to decrease error in our results. LIST OF SMALL SOURCES OF ERROR. With our time constraints, though, we feel we have struck a fair balance between efficiency and scientific rigor.

V. APPENDIX

A. Nuances of Error Analysis

[1] Note1 (????), we were not working with pure aluminum, so the critical temperature is higher than $1.2K$.

[2] Schmitt, R. W. (1961), "The Discovery of Electron Tunneling into Superconductors," *Physics Today*, 14, 38.

SIN I(V) Curve, Junction2

SIN I(V) Curve, Junction2

SIS I(V) Curve, Junction2

SIS I(V) Curve, Junction2

SIS I(V) Curve, Junction2

SIS I(V) Curve, Junction2